Raman probing of uniaxial strain in individual single-wall carbon nanotubes in a composite material

Dimitry Levshov, Yuri Yukzuk, Thierry Michel, Christophe Voisin, Laurent Alvarez, Sébastien Berger, Philippe Roussignol, Jean-Louis Sauvajol

Raman probing of uniaxial strain in individual single-wall carbon nanotubes in a composite material

D. I. Levshov[1], Yu. I. Yuzyuk[1], T. Michel[2],* C. Voisin[3], L. Alvarez[2], S. Berger[3], P. Roussignol[3], and J.-L. Sauvajol[2]

(1)- Faculty of Physics Southern Federal University, Rostov-on-Don, Russia

(2)- Laboratoire des Colloides, Verres et Nanomatériaux (UMR CNRS 5587), Université Montpellier 2, Place E. Bataillon, 34095 Montpellier, France

(3)- Laboratoire Pierre Aigrain (UMR CNRS 8551), Ecole Normale Supérieure, Université P. et M. Curie, Université D. Diderot, 24 rue Lhomond, 75005 Paris, France

E-mail: thierry.michel@univ-montp2.fr

*To whom correspondence should be addressed

Abstract

The temperature dependence of the Raman spectrum of a gelatine-based composite material doped with single-walled carbon nanotubes (SWNT@gelatin) is reported. A significant up-shift of the G-mode frequency is observed when the temperature is decreased from room temperature to 20 K. This frequency shift is significantly stronger than the one found for pure thermal effects. In contrast, the features of the radial breathing modes (frequencies and width) display no significant change in the same temperature range. These results are well understood by considering a uniaxial strain on the nanotube induced by the thermal expansitivity mismatch between the nanotube and the surrounding matrix.

Introduction

Since the time of their discovery in 1991,[1] carbon nanotubes have attracted a considerable interest in the research community and a lot of experimental and theoretical works has been devoted to their synthesis, properties and applications (see Ref.[2] and references therein). Due to their remarkable optical and electronic properties, carbon nanotubes are considered for promising applications in nano optoelectronic devices as transistors and diodes[3] or as nano emitter of light.[4] Because carbon nanotubes have also extraordinary tensile strength, they can potentially be used for creating high tensile strength fibers[5,6] and composites.[7]
Resonant Raman scattering (RRS) and photoluminescence (PL) spectroscopy have turned out to be the most valuable tools to investigate the coupling of nanotubes to their local environment.[2,8–10] Recently, the environmental effects on the optical properties of SWNTs in gelatin-based composite material were investigated by means of PL experiments.[11] The PL spectra of individual nanotubes embedded in gelatin showed a broadening and a global red shift of the PL lines with respect to PL experiments performed on micelle suspensions of the same nanotubes. More puzzling was the temperature dependence of the transition energies derived from PL and PLE (photoluminescence excitation) experiments of gelatin-based samples. A highly chiral dependent shift was observed upon cooling from 300 K to 20 K. The S_{11} transition (S_{11} is the first excitonic transition of a semiconducting SWNT) of type I semiconducting SWNTs (mod(2n+m;3) = 1) shows a negative shift in energy and a positive shift is measured on type II SWNTs (mod(2n+m;3) = 2). Shifts in opposite directions were found for the second excitonic transition, S_{22}. Variations of the band gap were theoretically predicted and experimentally observed when applying uniaxial strain on the nanotube.[12–14] This theoretical model turned out to be the suited framework to interpret the PL experimental results and the experimental temperature dependence of the S_{11} (S_{22}) transition of SWNTs embedded in gelatin was understood as due to the strain induced on SWNTs by the thermal expansion mismatch between the nanotube and the surrounding matrix.[11]

In this paper, we investigate the dependence as a function of temperature of the Raman spectrum of SWNTs in similar gelatin-based composite materials (hereafter called SWNT@gelatin). Raman spectroscopy allows comparison between the behaviors in temperature of metallic and semiconducting nanotubes embedded in gelatin, the former being inacessible in photoluminescence. In addition, the main Raman active phonon modes which are the radial breathing mode (RBM) and the tangential G-modes correspond to different atomic vibrations: normal vibration with respect to the wall of the tube for RBM and vibration into the wall of the tube for G-modes. By contrats to PL, the study of RBM and G-modes allows a fine investigation of the geometry of the deformation induced by the change in temperature on the nanotubes embedded in gelatin. Our main experimental findings are summarized as follows: a significant up-shift of the G-mode frequency for semiconducting as well as metallic SWNTs is observed when the temperature is decreased from room temperature (RT) to 20 K. In contrast, the radial breathing modes in SWNT@gelatin samples does not show any significant shift in the same temperature range. These results are well understood by considering an uniaxial compression induced on the nanotube by the thermal expansion mismatch between the nanotube and the surrounding gelatine at low temperature. Using theoretical predictions of the values of Grunesein parameters,[15] the temperature dependence of the frequencies of G-modes allows an evaluation of the average strain induced on the nanotubes by the temperature change.

Experimental details

Samples of gelatin-based composite material doped with either CoMoCat SWNTs (Sample I, SWNTs were produced by SouthWest Nanotechnologies) or HiPCO SWNTs (Sample II, SWNTs were purchased from Carbon Nanotechnologies Inc.) were prepared as follow. Isolated nanotubes encased in micelles of surfactant were obtained following standard methods[16] based on ultrasonication in an aqueous solution of Sodium Dodecyl Sulfate (SDS) (1wt %). After ultracentrifugation at 200000g for 4h, the supernatant was collected. As pointed by several studies, this method gives suspensions strongly enriched in isolated single nanotubes, but the suspension still contains a non negligible amount of small bundles.[17,18] For similar samples the relative amount of single tubes was estimated to be of the order of 10 %.[11] We further incorporated commercial dehydrated gelatin in the solution above the gelation temperature at 70°C (10 mg/ml). A little amount of this gelatin enriched solution was dropped on a quartz or copper substrate and solidifies at RT.
Resonant Raman scattering measurements in backscattering configuration were performed using a Jobin Yvon T64000 Micro Raman spectrometer equipped with a liquid nitrogen-cooled CCD detector. Four laser excitation energies were used: 2.41 eV (514.5 nm), 2.33 eV (532 nm), 1.70 eV (729 nm) and 1.58 eV (785 nm). The power density was kept around 3 kW/cm^2 for each wavelength.
An Oxford microstat was used to vary the sample temperature in small steps in the range 20 - 290 K.

Results

The radial breathing modes and G-mode regions of the resonant Raman spectra measured at 2.33 eV (532 nm) and 1.58 eV (785 nm) on the two different SWNT@gelatin samples are displayed in Figure 1 (left) at low and room temperature. The spectra show the same behavior for both samples and for the different excitations energies, namely : no significant shift of the RBM and a large up-shift of the G-modes when decreasing the temperature.

As can also be seen from Figure 1, the spectrum in the G-modes region shows two components, the so-called G^+ and G^- modes. As measurements were performed on an ensemble of disoriented nanotubes, the *A*, E_1 and E_2 modes contribute together at the Raman response of the G-mode even if the response of the *A* symmetry mode always dominates the spectrum.[21] For semiconducting SWNTs, the G^+-mode of *A* symmetry is associated with atomic vibrations along the tube axis (LO mode) and the G^--mode with vibrations normal to the tube axis (TO mode).[19] It must be underlined that the assignment of the G^+ and G^- modes is opposite for metallic SWNTs.[20] In the following, for each incident laser energy, E_{Laser}, G^+-band (G^--band) refers to the envelope of the G^+-modes (G^--modes) of different SWNTs in resonance condition with the incident laser photon, the so-called incident resonance: $E_{Laser}=E_{ii}$, (E_{ii} is an optical transition of a tube) or with the scattered photon, the so-called scattered resonance: $E_{Laser}-E_G=E_{ii}$ (E_G is the energy of the G-mode, it is close to 200 meV). Due to the higher intensity of the G^+-band in our spectra, we can use this latter as a probe to study the temperature dependence of an ensemble of LO (TO) modes of semiconducting (metallic) SWNTs embedded in gelatin.

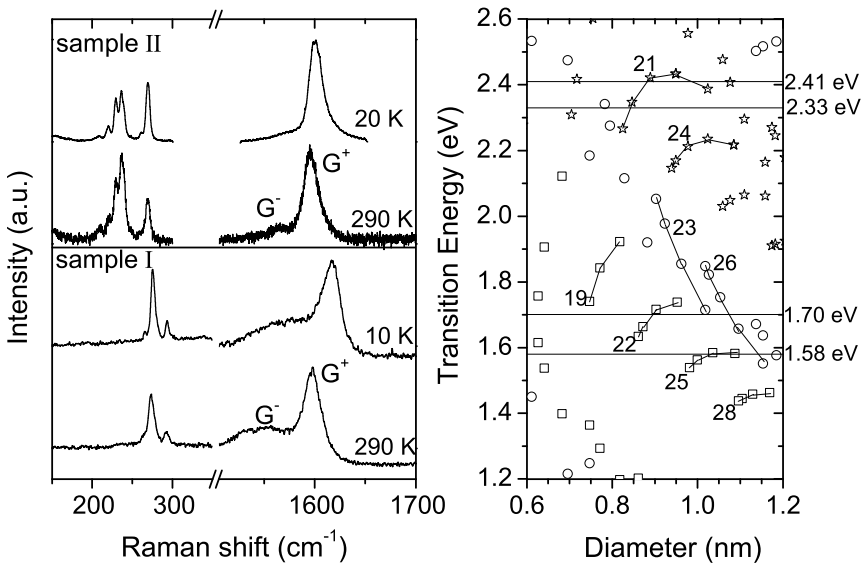

Figure 1: left: low and room temperature resonant Raman spectra measured on two SWNT@gelatin samples. The laser excitation energy is 2.33 eV for sample I, and 1.58 eV for sample II. Right: Kataura plot[23] in the S_{22} (SWNTs type I: open squares, SWNTs type II: open dots) and M_{11} (stars) regions. Excitation laser energies used in this work and 2n+m=const families are indicated on the figure.

Usually in Raman experiments performed on an ensemble on nanotubes, the identication of the (n,m) indices of nanotubes is done according to the procedure presented in Ref.[22] Briefly, the frequency of each component in the RBM range is related to a particular SWNT diameter using an appropriate RBM frequency vs. diameter relationship. In the present work we use the relationship: $\omega_{RBM} = \frac{215}{d} + 18$, derived from Raman experiments performed on individual SWNTs wrapped in surfactant.[22] By reporting these diameters in the Kataura plot derived from experimental results obtained for nanotubes dispersed in surfactants,[22,23] the (n,m) indices of nanotubes in incident resonance condition for each excitation energy, E_{Laser}, can be identified. This procedure request to measure the Raman excitation profile of a large number of RBMs to derive with a good accuracy the transition energies, E_{ii}, of a large number of nanotubes. In our experiments, only four excitation energies were available. In consequence we can only identify the nature (metallic or semiconducting), the order of the transition and the 2n+m=const families involved in each experiment as shown on the Kataura plot of the Figure 1 (right). For an excitation at 1.70 eV (1.58 eV), with regard to the frequencies of the RBM measured in each experiment on sample II, we state that the incident resonance condition $E_{Laser} = S_{22}$, occurs for semiconducting SWNTs belonging to the 2n+m=19, 22 and 23 families (22, 25 and 26 families), and these tubes mainly contribute to the Raman signal. In contrast, in Raman experiments performed on sample I by using the 2.33 eV and 2.41 eV laser excitation energies, we state that the incident resonance condition occurs for the metallic SWNTs belonging to the 2n+m=21 family ($E_{Laser}=M_{11}$, M_{11} is the first transition of metallic SWNT), and they contribute to the Raman signal together with a minor contribution of semiconducting tubes

belonging to the 2n+m =20 family. These assignments are in agreement with the profile of the G-modes on Figure 1. Indeed, as shown previously,[24,25] the profile of each G-mode is narrow and symmetric in semiconducting tubes as observed for sample II in Figure 1. By contrast, in chiral metallic tubes, a broad G^- band and a narrow G^+ are systematically found.[24,25] The presence of a broad G^- component for sample I in Figure 1 is a specific feature of chiral metallic SWNTs.

Regarding the G-modes, for the 2.33 eV excitation, the scattered resonance occurs for the 2n+m=24 metallic family and these tubes can also contribute to the signal in the G-mode range. Considering the usual diameter distribution in HiPCO samples, measured in this work at 1.58 eV and 1.70 eV, the 2n+m=28 family may contributes to the G-mode signal at 1.58 eV and we cannot totally exclude the scattered resonance of metallic tubes with diameter of about 1.5 nm at 1.70 eV (not shown on the Figure 1, right).

It must be underlined that the temperature dependence of the G^+-band features (frequency, width) measured on the two samples show the same kind of behaviour independently of the excitation energy and of the semiconducting or metallic nature of the tubes. As an illustration of the general features observed in all samples, we focus on the temperature dependence of the Raman spectrum of sample II measured at 1.70 eV (see Figure 2).

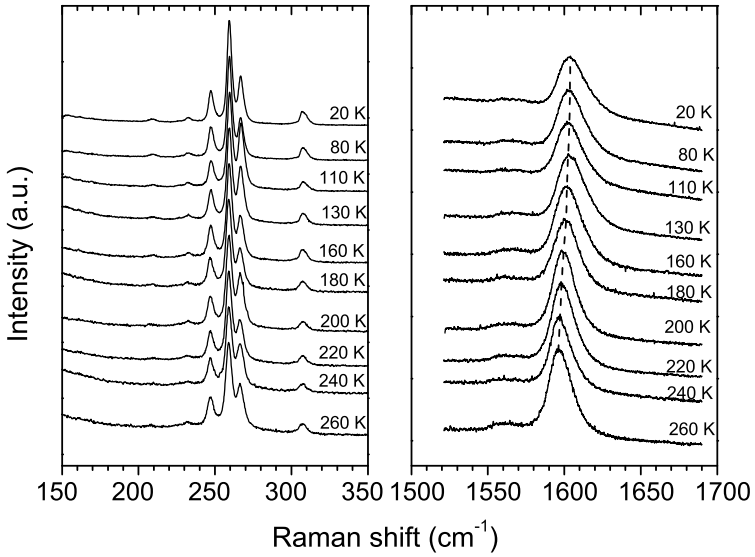

Figure 2: RBMs and G-modes ranges of the Raman spectra measured at 1.70 eV (sample II). For clarity, the spectra are normalized in intensity. The dashed line is a guide for the eyes.

As stated above, at the 1.70 eV excitation energy, only semiconducting tubes (specifically the 2n+m = 19, 22, 23 families) are in resonance on the S_{22} transition. Figure 3a shows the temperature dependence of the frequencies of the RBMs and G^+-band. The frequency of the different radial breathing modes does not change significantly in the whole temperature range investigated. More striking, the relative intensities of the RBM peaks do not significantly depend on temperature. This observation is in agreement with the small change in transition energy measured by PLE on the same sample[11] ($|\Delta S_{22}| \leq 20 meV$) which remains smaller than the width of the RBM resonance

window (ranging from 20 meV to 100 meV for individual SWNTs and small SWNTs bundles dispersed in surfactant[2]).

The frequency of G^+-band shift upward when decreasing the temperature. A linear temperature dependence of the G^+-band frequency was found from RT to about 60 K. The slope of this linear dependence is -0.047 cm^{-1}/K.

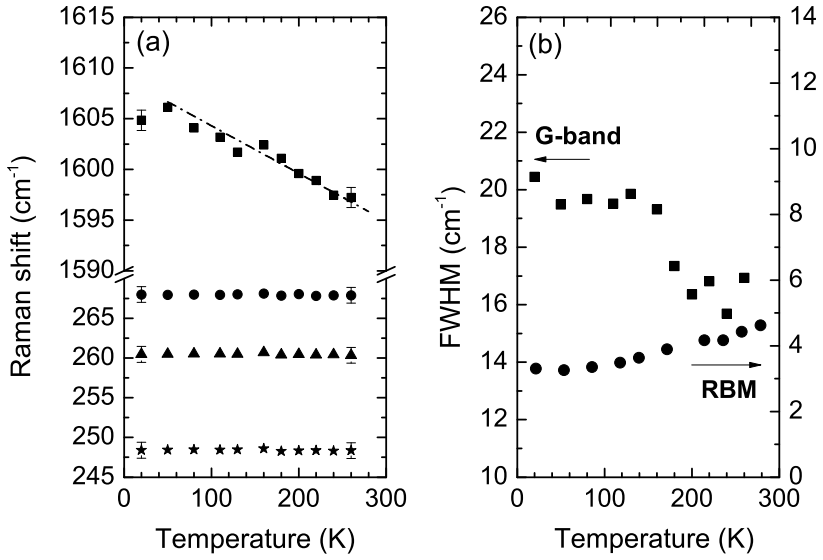

Figure 3: (a): temperature dependence of RBMs (dots, triangles, stars) and G-mode (squares) frequencies in SWNT@gelatin (sample II, E_{laser} = 1.70 eV). The dash-doted line is a linear fit of the data in the range 50 K - 260 K. (b): Temperature dependence of the FWHM of RBM (circles) and G^+mode (squares) for the sample II, E_{laser} = 1.70 eV.

The temperature dependence of the full width at half maximum (FWHM) of RBMs and G^+-band were analyzed. Conventional fitting procedure was used to determine the FWHM of these modes at all temperatures. A significant broadening of the G^+-band (from 5 to 10 cm^{-1}) together with a weak narrowing of RBMs' lines (of about 2 cm^{-1}) were observed on cooling (see Figure 3b). The decrease of anharmonic effects (phonon-phonon interactions) when decreasing the temperature usually leads to a narrowing of the modes as shown on RBM (Figure 3b). The expected narrowing of the line when decreasing the temperature is then opposite to the experimental behaviour measured on the G^+-band. This unusual and rather large broadening of the G^+-band can arise from change in the resonance conditions. Indeed, such change is usually responsible of the broadening of the Raman active modes.[26] However, this explanation is ruled out because the RBMs do not show a broadening when the temperature decreases indicating a very small change in the transition energies of the SWNTs under investigation in the whole temperature range. We then assume that the broadening of the G^+-band arises from inhomogeneous effects related to the contribution at the G^+-band of G-modes of different nanotubes with their own temperature dependence. This will be discussed in the next section.

Discussion

Regarding the temperature dependence of G^+-band frequency in SWNT@gelatin samples, a tentative explanation would be to assign this dependence to a thermal effect. This effect was studied in a film of bundles of SWNTs and usual up-shift of RBMs and G-mode frequencies was observed on cooling.[27,28]

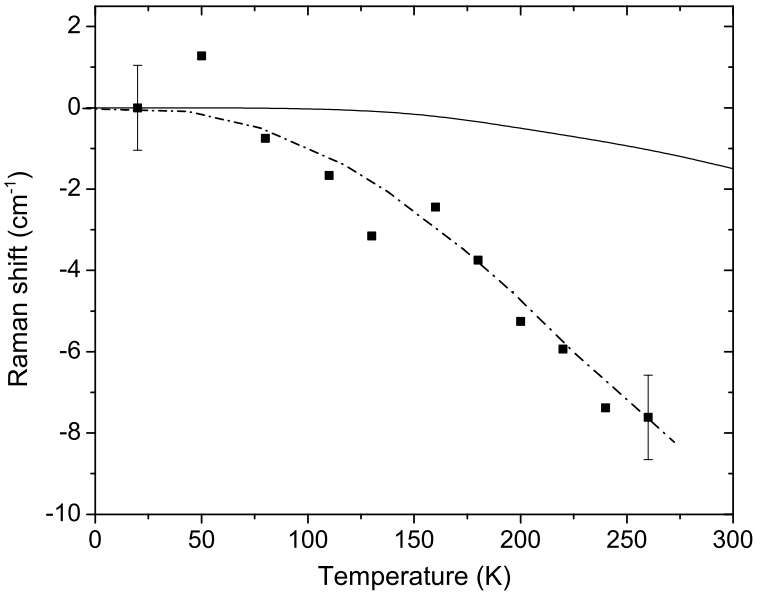

Figure 4: temperature dependence observed for the G-mode frequency shift ($\Delta\omega = \omega_{20K} - \omega_T$) in SWNT bundles (solid line: fit to the data from Ref.[27]) and in the SWNT@gelatin composite material (squares). The low-temperature frequency ω_{20K} is taken as reference to compare with results presented in Ref.[27] ω_T is the frequency at the temperature T. Dash-dotted line is a guide for the eyes.

Figure 4 shows the temperature dependence of the G-mode shift in SWNT@gelatin sample together with the one obtained on nanotube bundles.[27] Clearly, a simple thermal effect cannot explain the strong upshift measured in SWNT@gelatin sample on cooling. Moreover, as previously discussed, the broadening of the linewidth of the G-mode with decreasing the temperature is opposite to the expected narrowing of the phonons on cooling (see Figure 3b). These results definitively rule out pure thermal effect as the origin of the temperature dependence of the Raman spectra of SWNT@gelatin samples.

To understand these results, we must take into account environmental effects which are mainly related to the differences in the thermal expansivities of nanotubes and surrounding gel matrix (mostly due to water) as shown in Ref.[11]

The thermal expansion coefficient, α, is usually defined from the strain ε as :

$$\alpha = \frac{\varepsilon}{\Delta T}$$

It is of the order of $-5.10^{-6}K^{-1}$ for nanotubes[29] whereas for water ice it is slightly negative below

60 K and varies almost linearly from 0 at 60 K to $+4.10^{-5}K^{-1}$ at 200 K.[30] Since the composite material was synthetized above the gelation temperature, we assume that the matrix accomodates the nanotube shape at this temperature. In contrast cooling SWNT@gelatin to low temperatures ($\Delta T < 0$) results in a compression of the matrix inducing a compressive strain on the nanotubes.
Let's first assume that the stress applied to the nanotubes is hydrostatic. The dependence of the RBM and G-mode frequencies under hydrostatic pressure has been reported in several experimental[31–34] and theoretical works.[35,36] Comparing the average shift of the G^+-band (Figure 3, Figure 4) with the results of Merlen and co-workers (figure 4 in Ref.[34]) allows us to estimate an average value of the hydrostatic pressure induced on the nanotubes upon cooling the samples. For an average shift of the G^+-band of about 12 cm^{-1}, the stress should be on the order of 4 GPa. Such hydrostatic pressure should result in a frequency upshift of about 30 cm^{-1} for RBMs.[34] In contrast, no sizeable shift was found in SWNT@gelatin samples. Hence it rules out the effect of hydrostatic pressure in the temperature dependence of the RBM and G^+-band frequencies in SWNT@gelatin samples.
Recently the effect of uniaxial strain on the RBM and G-modes has been investigated experimentally[37,38] as well as theoretically.[15,39] It is known that for a positive uniaxial strain in the 0% - 10% range no shift of the RBM together with a significant linear down-shift of the G^+ and G^- modes were observed. These behaviors are close to those measured in SWNT@gelatin samples. Taking the experimental results of Bo Gao and coworkers[38] as reference and considering the average absolute shift of the G^+-band measured in our experiment between 290 K and 20K, we evaluated the absolute uniaxial strain applied on the nanotubes to be close to 1 %. Let us emphasize that in SWNT@gelatin samples, decreasing the temperature from RT to low temperature is equivalent to applying a compressive strain on the nanotubes. Conversely, the experiment is equivalent to apply a tensile strain when the temperature increases from low temperature to RT. In the framework of this assumption, the broadening of G mode (Figure 3b) with decreasing temperature may be due to sampling of many types of SWNTs with varying degree of strain.

Our experimental evaluation of the uniaxial strain is also in agreement with the theoretical calculations of Wu and co-workers[15] who predict a down-shift of the G-modes under tensile strain. In the same papers, the Gruneisen parameters of different modes of nanotubes are calculated and their use here allows to compare our experimental results with theoretical predictions.
Usually the mode's Gruneisen parameter is defined as:[40]

$$\frac{\omega_j(P)}{\omega_j(0)} = \left(\frac{V(P)}{V(0)}\right)^{-\gamma_j} \tag{1}$$

where γ_j is the j-mode's Gruneisen parameter, $\omega_j(P)$ ($\omega_j(0)$) is the frequency of the j-mode under (without) pressure P and $V(P)$ ($V(0)$) is the volume of the unit cell under (without) pressure.
We can adapt the previous equation to our one dimensional system in order to obtain a relationship between the uniaxial compressive strain ε=ΔL/L, and the G^+-band frequency. Since the RBM frequency does not change in our experiment (implying that the tube diameter almost does not change under compressive strain), the previous equation leads to:

$$\frac{\Delta L}{L} = \left(\frac{\omega_0}{\omega_T}\right)^{\frac{1}{\gamma_G}} - 1 \tag{2}$$

where γ_G is the Gruneisen parameter of G-mode and $\omega(T)$ is the frequency of the G^+-band at a given temperature T below RT, and ω_0 is the G^+-band frequency at RT when the nanotube is relaxed. In order to evaluate the uniaxial strain, we assume the Gruneisen parameter of LO G^+ mode in chiral semiconducting and TO G^+ mode in metallic SWNTs to be close of 0.9.[15] Under this assumption, we find an absolute uniaxial strain of 1 % in good agreement with the experimental evaluation on the basis of results presented in Ref.[38] A similar value of the strain is found for all the excitation energies used in this work independently of the semiconducting or metallic character of the tubes.

The Poisson ratio ν for SWNTs, is usually defined by $\frac{D^*-D}{D} = -\nu\varepsilon$ (D^* and D are the diameter under and without strain, respectively). The Poisson ratio value was found to be close to 0.2 in individual nanotubes.[41] A strain of 1 % induces a very small change in the SWNTs' diameter ($D^* = 0.998D$) and consequently a non-significant change in the RBM frequencies under strain as experimentally observed.

Assuming the nanotube's Young modulus to be 1 TPa, a strain of 1 % corresponds to an applied uniaxial pressure of about 10 GPa. It can be pointed out that this value of the applied uniaxial pressure is in fair agreement with the one obtained from PL measurements (7.5 GPa).[11]

This set of experimental observations indicates that there is a good mechanical load transfer from the matrix to the nanotubes: the matrix does not accommodate the new nanotube length by internal deformation and on the contrary most of the length mismatch is absorbed by the nanotube.

Another strong conclusion of this study confirming results from PL measurements is that the strain induced on the nanotubes is definitively uniaxial. This result is not intuitive for an isotropic medium and stems from the quasi one-dimensional aspect of the tubes.[42]

We propose that this effect comes from nanoscale imperfections of the interface between the nanotube and the matrix. Along the tube axis, where the absolute strain is large ($|\Delta L| = L\alpha_m\Delta T$ where α_m is the thermal expansion coefficient of the matrix), this imperfection is completely negligible and most of the strain is transferred to the tube, whereas in the perpendicular direction the very small dilatation ($\Delta e = e\alpha_m\Delta T \sim 10^{-3}\Delta L$) remains small or comparable to the imperfection scale preventing a good coupling between the matrix and nanotube deformations.

Conclusion

In this paper we have discussed the temperature dependence of the Raman spectrum of a gelatine-based composite material doped with single-walled carbon nanotubes (SWNT@gelatin). The significant up-shift of the G-mode frequency when decreasing the temperature from RT to 20 K, regardless of the metallic or semiconducting character of nanotubes, is well understood by considering an uniaxial compressive strain on the nanotube induced by the thermal expansitivity mismatch between the nanotube and the surrounding gelatin. This point is not intuitive for nanotubes dispersed in gelatin, since one would rather expect an isotropic strain. Such effect is related to the aspect ratio of nanotubes and emphasizes their extreme sensitivity to the environment. Finally, we propose that same experiments performed on other one-dimensional nanostructures, such as double-walled carbon nanotubes or peapods, embedded in gelatin provide a simple approach to investigate their vibrational properties under strain.

Acknowledgements

The authors acknowledge financial support from grant RFBR 09-02-91076 CNRS and French Russian PICS N^0 4818.

References

(1) S. Iijima, Nature **354**, 56 (1991).

(2) A. Jorio, M. S. Dresselhaus, and G. Dresselhaus, *Carbon nanotubes: Advanced Topics in the Synthesis, Structure, Properties and Applications* (Springer Series on Topics in Appl. Phys. 111 Springer Verlag, Berlin, 2008).

(3) P. Avouris, *et al.*, Nature Nanotechnology **2**, 605 (2007).

(4) T. Mueller, *et al.*, Nature Nanotechnology **5**, 27 (2010).

(5) B. Vigolo, *et al.*, Science **290**, 1331 (2000).

(6) K. Koziol, *et al.*, Science **318**, 1892 (2007).

(7) J.N. Coleman, *et al.*, Carbon **44**, 1624 (2006).

(8) M. Steiner, *et al.*, Appl. Phys. A **96**, 271 (2009).

(9) S. Chiashi, *et al.*, Nano. Lett. **8**, 3097 (2008).

(10) P. T. Araujo, *et al.*, Phys. Rev. Lett. **103**, 146802 (2009).

(11) S. Berger, *et al*, Journal of Applied Phys. **105**, 094323 (2009).

(12) L. Yang, *et al.*, Phys. Rev. B**60**, 13874 (1991) .

(13) L. Yang, *et al.*, Phys. Rev. Lett. **85**, 154 (2000).

(14) Huang, *et al.*, Phys. Rev. Lett. **100**, 136803(2008).

(15) G. Wu, *et al.* Phys. Rev. B *72*, 115411 (2005).

(16) M.J. O'Connell, *et al*, Science **297**, 1 (2002).

(17) P.H. Tan, *et al.*, Phys. Rev. Lett. **99**, 137402 (2007).

(18) S. Berger, *et al.*, Nano. Lett. **7**, 398 (2007).

(19) S. Reich, C. Thomsen, and J. Maultzsch, *Carbon nanotubes: Basic Concepts and Physical Properties*, (Wiley-VCH, Weinheim, Germany, 2004).

(20) S. Piscanec, *et al.*, Phys. Rev. B **75**, 035427 (2007).

(21) M. S. Dresselhaus *et al.*, Carbon **40**, 2043 (2002).

(22) J. Maultzsch, *et al.*, Phys. Rev. B **72**, 205438 (2005).

(23) A. Jorio, *et al.*, Phys. Rev. B **71**, 075401 (2005).

(24) M. A. Pimenta, *et al.*, Phys. Rev. B **58**, R16016 (1998).

(25) T. Michel, *et al.*, Phys. Rev. B **80**, 245416 (2009).

(26) A. Jorio *et al.*, Phys. Rev. B **66**, 115411 (2002).

(27) K. Gao, *et al.*, J. Phys. Cond. Matter **19**, 486210 (2007).

(28) N. R. Raravikar, *et al*, Phys. Rev. B **66**, 235424 (2002).

(29) Y.K. Kwon, *et al.*, Phys. Rev. Lett. **92**, 015901 (2004).

(30) H. Tanaka, J. Mol. Liq. **90**, 323 (2001).

(31) U. D. Venkateswaran, *et al.*, Phys. Rev. B **59**, 10928 (1999).

(32) U. D. Venkateswaran *et al.*, Phys. Rev. B **68**, 241406 (R) (2003).

(33) P. Teredesai, *et al.*, Phys. Stat. Sol. B **223**, 479 (2001).

(34) A. Merlen, *et al.* Phys. Rev. B **72**, 035409 (2005).

(35) L. Chernozatonskii, *et al.*, Phys. Rev. B **65**, 241404 (R) (2002).

(36) S. Reich, *et al.*, Phys. Stat. Sol. B **235**, 354 (2003).

(37) S. B. Cronin, *et al.*, Phys. Rev. Lett. **93**, 167401 (2004).

(38) Bo Gao, *et al.*, J. Phys. Chem. C **112**, 20123 (2008).

(39) Wei Yang, *et al.*, Phys. Rev. B **77**, 195440 (2008).

(40) B. Weinstein and R. Zallen, in Light Scattering in Solids, edited by M. Cardona and G. Guntherodt, Springer, Vol. IV, Berlin (1984).

(41) J. Cao, *et al.*, Phys. Rev. Lett. **90**, 157601 (2003).

(42) J. R. Wood, *et al.*, J. Phys. Chem. B *103*, 10388 (1999).